

\mathcal{PT} -systems without parity symmetry: topological states, hidden symmetry, and the \mathcal{PT} phase diagram

Yogesh N. Joglekar

Department of Physics, Indiana University Purdue University Indianapolis (IUPUI), Indianapolis, Indiana 46202, USA
(Dated: January 27, 2023)

\mathcal{PT} -symmetric systems, until now, have been characterized by a real, parity-symmetric, kinetic Hamiltonian and a non-Hermitian, balanced gain-loss potential. We present a new class of discrete models in which the tunneling Hamiltonian is not parity-symmetric, and yet the models have a nonzero \mathcal{PT} -breaking threshold in presence of a pair of gain-loss impurities $\pm i\gamma$ located at reflection-symmetric sites. We uncover a hidden symmetry that is instrumental to the finite threshold strength. We show that such models have topological edge-states that remain robust in the \mathcal{PT} -broken phase. Our predictions substantially broaden possible realizations of a \mathcal{PT} system, particularly in optical waveguide arrays or coupled microstructures, by eliminating the parity-symmetry constraint.

Introduction. When is the spectrum of a non-Hermitian Hamiltonian purely real or has only complex-conjugate pairs? Numerous authors have addressed this question, starting with Bender and coworkers who showed that (continuum) Hamiltonians invariant under combined parity- and time-reversal operations (\mathcal{PT} symmetric) fit the bill [1–3]. Such Hamiltonians faithfully model open systems with balanced gain and loss, in which the parity operator (\mathcal{P}) exchanges the gain-region with the loss-region, whereas the time reversal operator (\mathcal{T}) transforms a gain-region into a lossy region. Concurrent with their experimental realizations in coupled waveguides [4–8], resonators [9], microcavities [10], and lasers [11–14], discrete \mathcal{PT} systems with a parity-symmetric tunneling term $H_0 = \mathcal{P}H_0\mathcal{P} = H_0^\dagger$ and a gain-loss potential $V = \mathcal{PT}V\mathcal{PT} \neq V^\dagger$ have been intensely studied in the past five years [15–20]; in particular, site-dependent tunneling Hamiltonians, of interest for perfect-state-transfer and quantum computing [21], have been theoretically [22] and experimentally [23] explored. All of these systems are subject to the stringent parity-symmetry requirement for the tunneling amplitude profile.

Generically, the spectrum of a \mathcal{PT} -symmetric Hamiltonian $H = H_0 + V$ is real when the strength γ of the balanced gain-loss potential is smaller than a positive threshold γ_{PT} set by H_0 . The emergence of complex-conjugate eigenvalues at the exceptional point $\gamma = \gamma_{PT}$ is called \mathcal{PT} -symmetry breaking [24, 25]. When $\gamma > \gamma_{PT}$, the eigenfunctions with complex eigenvalues become increasingly asymmetrical [26]. It has long been known that a purely real or complex-conjugate-pairs spectrum is equivalent to the existence of an antiunitary operator $O = U\mathcal{T}$ that commutes with the Hamiltonian H [27–29]. Thus, in principle, parity symmetry is not a necessary constraint, $U \neq \mathcal{P}$. Nonetheless, in practice, all physically realizable models have abided by it, $U = \mathcal{P}$.

This observation begs the question: Do physically realizable systems without parity symmetry, that undergo a transition from purely-real to complex-conjugate-pairs spectrum exist? *In this paper, we show that the answer to this question is affirmative.* By explicit construction of lattice models with periodic, asymmetrical tunneling

profile and a positive transition threshold, we also elucidate the hidden spatial-symmetry properties of such systems. Our results, thus, substantially broaden the possible realizations of systems with balanced gain and loss. Therefore, in this context, we continue to use the terms “ \mathcal{PT} -systems” and “ \mathcal{PT} -transition” even in the absence of parity symmetry.

Consider an N -site tight-binding lattice with site-dependent tunneling $t_k = J[1 + \lambda \cos(2\pi\beta k + \phi)] = t_k^*$ and a pair of gain-loss potentials $\pm i\gamma$ located at parity-symmetric sites m_0 and $\bar{m}_0 = N + 1 - m_0$ respectively. Here $J > 0$ denotes the energy scale associated with the tunneling rate. Since the general tunneling function is not parity (and \mathcal{PT}) symmetric, $t_k^* \neq t_{N-k}$, this lattice model is not \mathcal{PT} symmetric, although the non-Hermitian potential is. Hermitian tight-binding lattices with tunneling profile t_k have been extensively studied due to their connections with the Su-Schrieffer-Heeger (SSH) model [30, 31], the Hofstadter-butterfly problem [32], and the diagonal, incommensurate Aubry-Andre Harper model of one-dimensional quasicrystals [33–36]. This lattice model with a rational β has robust topological edge states [37] and is related to topological insulators [38–41].

Our three primary results are as follows. i) Although not \mathcal{PT} -symmetric, this model has a positive threshold $\gamma_{PT}(m_0, \phi) > 0$ when $\beta = 1/p$, lattice size $N = Mp - 1$, and gain-potential site-index $m_0 = Kp$ where p, M, K are positive integers. ii) For $\gamma \leq \gamma_{PT}$ the eigenfunctions show a hidden reflection symmetry, $|f(j)| = |f(N+1-j)|$, only when restricted to sites $j = \{p, 2p, \dots\}$. This symmetry is destroyed when the threshold is exceeded. iii) The model has $p - 1$ localized edge modes, interspersed among its p bands, that continue to have real energies past the \mathcal{PT} -transition.

In the following paragraphs, we first present the properties of the parity-asymmetrical tunneling Hamiltonian, followed by the \mathcal{PT} phase diagram as a function of four parameters $(\lambda, \beta, \phi; m_0)$ that characterize the system. We then discuss a hidden symmetry that leads to the positive \mathcal{PT} threshold even in the presence of an asymmetrical tunneling. We conclude the paper with a brief discussion.

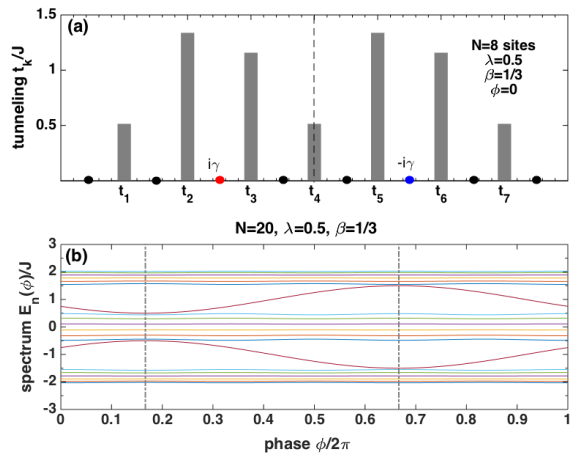


FIG. 1. (Color online): (a) Schematic of a lattice with $N = 8$ sites, denoted by solid circles, and *parity-asymmetric* tunneling amplitude t_k/J . Also shown are balanced gain-loss potentials $\pm i\gamma$, denoted by red and blue solid circles respectively, at parity symmetric sites; the vertical dashed line is the lattice center. (b) Spectrum $E_n(\phi)$ of an $N = 20$ lattice ($\gamma = 0$) shows $1/\beta = 3$ bands, each with $[N\beta] = 6$ extended states. The two remaining mid-gap states are localized.

Tight-binding model. The Hermitian tunneling Hamiltonian for an N -site lattice is given by

$$H_0(\lambda, \beta, \phi) = - \sum_{k=1}^{N-1} t_k(|k\rangle\langle k+1| + |k+1\rangle\langle k|), \quad (1)$$

where $|k\rangle$ denotes a single-particle state localized at site k . The action of the parity operator on a lattice is given by $\mathcal{P} : t_k \rightarrow t_{N-k}$. The Hamiltonian $H_0(\lambda, \beta, \phi)$ is not, in general, invariant under the \mathcal{PT} operation; the trivial exceptions are a uniform lattice, $\lambda = 0$, or an SSH model with even N .

Since the tunneling function $t_k(\lambda, \beta, \phi)$ is periodic in β and ϕ , it is sufficient to consider $\beta \in [0, 1)$ and $\phi \in [0, 2\pi)$. It is also straightforward to show that $H_0(-\lambda, \beta, \phi) = H_0(\lambda, \beta, \phi + \pi)$ and $H_0(\lambda, 1 - \beta, \phi) = H_0(\lambda, \beta, 2\pi - \phi)$. Therefore, it is sufficient to restrict ourselves to $\lambda \geq 0$ and $\beta \leq 1/2$. The general band structure of the Hamiltonian $H_0(\lambda, \beta, \phi)$ is highly intricate, where the number of bands is determined by β , and the locations of band degeneracies are determined by λ and ϕ [32–37]. Note that when $\lambda \geq 1$, the tunneling amplitude t_k changes sign from positive to negative along the lattice. In addition, for $\lambda \geq 1$ and a rational $\beta = q/p$, the tunneling amplitude vanishes at $k = Mp$ and $\phi = \arccos(-1/\lambda)$. For such parameters, the N -site chain is split into pieces of size p , and the corresponding Hamiltonian H_0 becomes block-diagonal. In order to avoid the complexities that arise for $\lambda \geq 1$, initially, we confine ourselves to modulation strengths $0 \leq \lambda < 1$.

In the presence of gain-loss potentials $\pm i\gamma$ at parity-symmetric sites m_0 and \bar{m}_0 , the lattice Hamiltonian be-

comes $H = H_0 + V$ with

$$V = i\gamma (|m_0\rangle\langle m_0| - |\bar{m}_0\rangle\langle \bar{m}_0|) = \mathcal{PTVPT} \neq V^\dagger. \quad (2)$$

Figure 1 encapsulates the typical properties of Hamiltonian H_0 . Panel (a) shows the parity-asymmetric tunneling profile t_k/J for an $N = 8$ site lattice with tunneling modulation strength $\lambda = 0.5$, inverse tunneling period $\beta = 1/3$, and phase $\phi = 0$. The neutral sites on the lattice are indicated by solid black circles, the solid red circle at $m_0 = 3$ denotes the gain site, and the loss site at its parity-symmetric location $\bar{m}_0 = 6$ is denoted by the solid blue circle. Panel (b) shows the energy spectrum $E_n(\phi)$ for an $N = 20$ site lattice with Hamiltonian H_0 . In addition to the three bands of extended states that are expected at $\beta = 1/3$, there are two edge-localized states with energies that lie in the two band-gaps. The midgap states are localized for all ϕ except $\phi = \{\pi/3, 4\pi/3\}$, denoted by dotted vertical lines.

These are generic features of the spectrum for inverse tunneling period $\beta = 1/p$ and lattice sizes $N = Mp - 1$. Each of the p bands has $[N\beta] = (M - 1)$ extended states, and the remaining $(p - 1)$ midgap states are localized for almost all ϕ . When $N = Mp - 1$, it is straightforward to show that $\mathcal{PT}H_0(\lambda, \beta, \phi)\mathcal{PT} = H_0(\lambda, \beta, 2\pi\beta - \phi)$. Thus, H_0 becomes \mathcal{PT} symmetric only at $\phi = \{\pi\beta, \pi\beta + \pi\}$; these are precisely the ϕ -values at which the midgap states become extended. In the following, we will see that these topological midgap states do not participate in the \mathcal{PT} breaking and retain their localized character past the \mathcal{PT} transition.

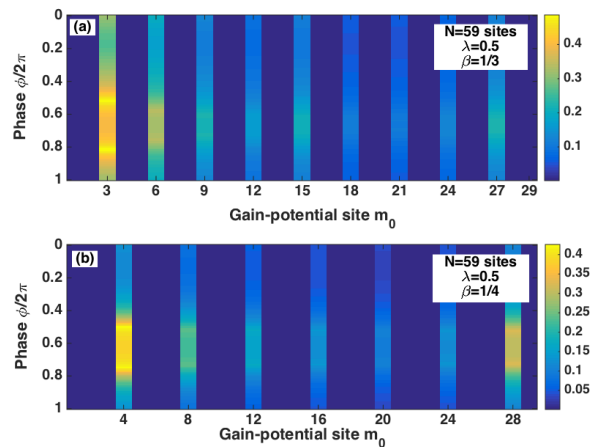


FIG. 2. (Color online): \mathcal{PT} threshold γ_{PT}/J as a function of gain-site index $1 \leq m_0 \leq N/2$ and ϕ for an $N = 59$ lattice with parity asymmetric tunneling. (a) For $\beta = 1/3$, $\gamma_{PT} = 0$ for all gain locations except $m_0 = \{3, 6, \dots\}$. (b) When $\beta = 1/4$, a positive γ_{PT} is obtained when $m_0 = \{4, 8, \dots\}$. These results show that, contrary to naive expectations, a parity-asymmetric tunneling Hamiltonian with a \mathcal{PT} -symmetric potential has a positive, tunable threshold $\gamma_{PT}(m_0, \phi)/J \sim 1 > 0$.

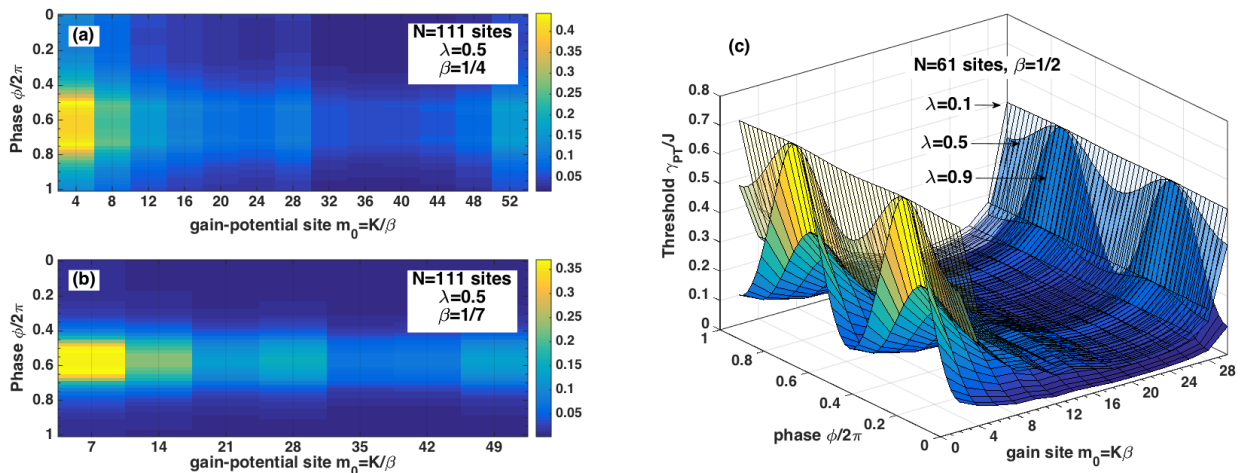


FIG. 3. (Color online): Dependence of the \mathcal{PT} threshold $\gamma_{PT}(m_0, \phi)/J$ on the tunneling modulation period $1/\beta$ and modulation strength λ . (a) $\gamma_{PT}(m_0, \phi)$ for an $N = 111$ lattice shows that it is largest for gain-loss sites that are farthest from ($m_0 = 4$) or closest to ($m_0 = 52$) each other. (b) shows the same qualitative behavior for the same lattice, $N = 111$ with a larger tunneling modulation period $1/\beta = 7$. In both cases, γ_{PT} has a nontrivial phase dependence. (c) shows that as modulation strength λ increases, the threshold γ_{PT} is monotonically suppressed from its value in the $\lambda \ll 1$ limit. The results in panel (c) are for an $N = 61$ lattice with $\beta = 1/2$.

\mathcal{PT} phase diagram. We now present the \mathcal{PT} phase diagram for this model. Naively, the parity asymmetric nature of the tunneling Hamiltonian H_0 , Fig. 1, implies that an infinitesimal gain-loss potential, Eq.(2), should lead to a \mathcal{PT} transition and a complex spectrum. This expectation is indeed confirmed by numerical results for all lattice sizes N except when $N = Mp - 1$.

Figure 2 shows the \mathcal{PT} threshold strength γ_{PT}/J in the (m_0, ϕ) plane for lattice size $N = 59$ and tunneling modulation strength $\lambda = 1/2$. Panel (a) shows that for $\beta = 1/3$, the threshold is zero except when the gain location is an integer multiple of the tunneling period, $m_0 \propto 1/\beta = 3$; panel (b) shows that a similar behavior is obtained for $\beta = 1/4$. In general, the nonzero threshold γ_{PT}/J first decreases as the gain-potential site m_0 moves in from the end of the lattice and increases again as it approaches the lattice center, $m_0 \rightarrow N/2$ [42]. These results are qualitatively similar for large N and the maximum threshold strength remains the same in the thermodynamic limit, $M \gg 1$.

Figure 3 shows the typical dependence of positive γ_{PT} on the tunneling period $p = 1/\beta$ and tunneling modulation strength λ ; in each case, only gain-potential locations $m_0 \leq N/2$ that give rise to a positive \mathcal{PT} threshold, $m_0 \propto p$, are considered. Panels (a) and (b) show the \mathcal{PT} threshold in the (m_0, ϕ) plane for the same modulation strength $\lambda = 1/2$ and lattice size $N = 111$. Consistent with the results in Fig. 2, the \mathcal{PT} threshold varies non-monotonically with phase ϕ , and is generally maximum when the gain and loss locations are farthest apart or nearest to each other. As the tunneling period is increased from $1/\beta = 4$, panel (a), to $1/\beta = 7$, panel (b), we see that the region with appreciable threshold value

shrinks in size, but the maximum value of γ_{PT} does not alter substantially.

Panel (c) in Fig. 3 shows the dependence of the \mathcal{PT} threshold $\gamma_{PT}(m_0, \phi)$ on λ for a lattice with $N = 61$ sites and $\beta = 1/2$. When $\beta = 1/2$, the tunneling amplitude on adjacent bonds alternates between two values $J(1 \pm \lambda \cos \phi)$ [30, 31], and for an odd N the tunneling profile is not parity symmetric. At $\lambda = 0.1$, due to the small tunneling modulation, the threshold γ_{PT} is essentially independent of the phase ϕ , and its dependence on m_0 is similar to that for a uniform tunneling lattice; in particular, we see that $\gamma_{PT}/J \rightarrow 0.5$ when the gain and loss sites are closest to each other [42]. As λ increases, the \mathcal{PT} threshold, which is proportional to the effective tunneling amplitude, is strongly suppressed when $\cos \phi = \pm 1$, but remains unchanged from its $\lambda \ll 1$ limit when $|\phi| \approx \pi/2$. As an aside, we note for $\beta = 1/p < 1/2$, the ϕ -dependence of the threshold γ_{PT} is not as easily characterized. Results in Figs. 2 and 3 might suggest that the threshold for farthest gain and loss, $\gamma_{PT}(p, \phi)$, reaches a maximum at $\phi = \{\pi, \pi + \pi\beta\}$; however, that is not true for all modulation strengths $\lambda < 1$.

Figs. 2 and 3 encapsulate global features of the \mathcal{PT} phase diagram and its dependence on four parameters, three of them related to the parity asymmetric tunneling, (λ, β, ϕ) and the fourth, m_0 , related to the balanced gain-loss potential. Although the detailed structure of the \mathcal{PT} threshold manifold $\gamma_{PT}(m_0, \phi)$ depends on the other two parameters, it is clear that the γ_{PT} is maximum when the gain and loss sites are either closest to each other or farthest away.

Origin of the positive threshold. Let us recall how a positive \mathcal{PT} breaking threshold arises in the traditional \mathcal{PT} -

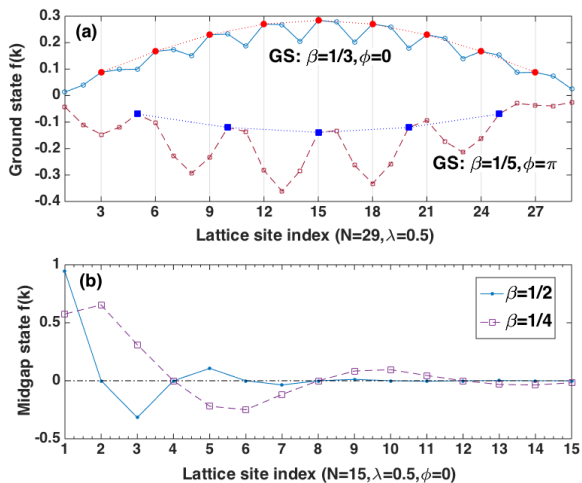


FIG. 4. (Color online): Hidden symmetry of eigenfunctions of the parity asymmetric tunneling Hamiltonian $H_0(\lambda, \beta, \phi)$. (a) $N = 29$ lattice shows *parity asymmetric* ground states (solid and dashed lines). However, these states have parity-symmetric amplitudes on sites $k \propto 1/\beta$ (red solid circles, blue solid squares). (b) lowest energy midgap edge-states for an $N = 15$ lattice with $\beta = \{1/2, 1/4\}$ show that their wavefunctions vanish at sites $k \propto 1/\beta$; the states, thus, are unaffected by the balanced gain-loss potential.

symmetric Hamiltonians. If the tunneling Hamiltonian is \mathcal{PT} -symmetric, so are its eigenfunctions $f_\alpha(k)$ with energies ϵ_α . Therefore, in the presence of a \mathcal{PT} symmetric potential, Eq.(2), the first-order perturbative correction to the energy, $\Delta_\alpha^1(\gamma) = i\gamma(|f_\alpha(m_0)|^2 - |f_\alpha(\bar{m}_0)|^2)$, as well as all higher odd-order corrections vanish, $\Delta_\alpha^{2k+1}(\gamma) = 0$ [43]. This property ensures a real spectrum $\epsilon_\alpha(\gamma)$ for potential strength $\gamma \leq \gamma_{PT}$.

But what if H_0 is not reflection-symmetric? Its arbitrary eigenstate $f_\alpha(k)$ with energy ϵ_α satisfies the following difference equations at parity-symmetric sites ($k, \bar{k} = N + 1 - k$)

$$t_{k-1}f_\alpha(k-1) + t_k f_\alpha(k+1) = -\epsilon_\alpha f_\alpha(k), \quad (3)$$

$$t_{\bar{k}-1}f_\alpha(\bar{k}-1) + t_{\bar{k}} f_\alpha(\bar{k}+1) = -\epsilon_\alpha f_\alpha(\bar{k}), \quad (4)$$

where open boundary conditions are implemented by using $t_0 = 0 = t_N$. It follows then that if $t_k \neq t_{\bar{k}-1}$, the eigenfunctions, in general, will not have equal weights on the parity symmetric sites, $|f_\alpha(k)| \neq |f_\alpha(\bar{k})|$. Figure 4 shows typical eigenfunctions of Hamiltonian H_0 when the lattice size satisfies $N = Mp - 1$. Panel (a) in Fig. 4 shows the ground-state (GS) wavefunctions $f(k)$ for an $N = 29$ site lattice with $\beta = 1/3$ (solid line with open circles) and $\beta = 1/5$ (dashed line with open squares). As is expected, both are asymmetrical about the center site, $n_c = 15$. However, these wavefunctions have a *hidden symmetry*: solid red circles show the $\beta = 1/3$ GS amplitudes at sites $k \propto p = \{3, 6, \dots\}$, whereas the solid blue squares show the $\beta = 1/5$ GS amplitudes at sites $k \propto p = \{5, 10, \dots\}$. In both cases the wavefunction sat-

isfies $|f_\alpha(m_0)| = |f_\alpha(\bar{m}_0)|$ if and only if m_0 is an integer multiple of the tunneling modulation period $1/\beta$. This result is true for all eigenstates of $H_0(\lambda, \beta, \phi)$ as long as the lattice size satisfies $N = Mp - 1$. It ensures that the counterpart site index $\bar{m}_0 = N + 1 - m_0$ is also an integer multiple of the tunneling modulation period. This hidden symmetry is instrumental to a positive \mathcal{PT} threshold that we observe when the gain potential is located at sites $m_0 \propto p = 1/\beta$. It also implies that the eigenfunctions of the total Hamiltonian $H = H_0 + V$ continue to have this symmetry for $\gamma \leq \gamma_{PT}$.

Panel (b) shows the lowest energy midgap state for an $N = 15$ lattice with $\beta = 1/2$ (solid line) and $\beta = 1/4$ (dashed line); these states are localized at one end of the lattice. The surprising feature, shared by both states, is the presence of nodes precisely at sites $m_0 = \{p, 2p, \dots\}$. When the lattice size is $N = Mp - 1$, due to the tunneling asymmetry at the two ends of the lattice, it follows that a midgap state must be localized at one end or the other, but not equally at both ends. Therefore, the hidden symmetry discussed in the previous paragraph implies that its wavefunction must vanish at sites $m_0 \propto p = 1/\beta$. This result is true for all $(p - 1)$ localized midgap states. This remarkable property of the localized states implies that a balanced gain-loss potential, Eq.(2), has no effect on them. In particular, the energies of these states remain real and these localized, topological states [37] remain robust when the \mathcal{PT} breaking strength exceeds the threshold, $\gamma > \gamma_{PT}(\lambda, \beta, \phi; m_0)$. In recent years, the presence or absence of topological insulator states in \mathcal{PT} -symmetric Dirac and SSH models has been extensively studied [38–41]. Our results show that robust, topological states occur in a wide class of \mathcal{PT} asymmetric Hamiltonians that, surprisingly, have a positive \mathcal{PT} threshold.

Finally, let us dispense with one special case: the SSH model with even N . In contrast to the odd N case, when N is even, the Hamiltonian H_0 is always \mathcal{PT} symmetric. Its spectrum $E_n(\phi)$ has a pair of zero-energy states symmetrically localized at two ends of the lattice when $|\phi| \leq \pi/2$ [30, 31, 37]. Therefore, we find $\gamma_{PT} = 0$ when the degenerate, topological, edge-states are present, i.e. $|\phi| \leq \pi/2$, and that $\gamma_{PT} > 0$ when they are absent, i.e. $\pi/2 < \phi < 3\pi/2$.

Discussion. In this paper, we have discovered a broad class of Aubry-Andre Harper models [37] with *parity asymmetric tunneling* that have a positive \mathcal{PT} threshold when the lattice size N , the tunneling modulation period $1/\beta = p$, and the gain-potential location m_0 are related by $N = Mp - 1$ and $m_0 = Kp \leq N/2$. By eliminating the reflection symmetry constraint, these models substantially broaden possible experimental realizations of a system that undergoes a “ \mathcal{PT} transition”, even in the absence of the parity symmetry.

Our results also apply for any rational $\beta = q/p \leq 1/2$ with $q > 1$. In all such cases, the threshold γ_{PT} is positive only when $N = Mp - 1$ and $m_0 = Kp$; otherwise, it is zero. The sole exception to this rule is the finite, dis-

crete set of $\phi \in [0, 2\pi)$ values that satisfy $2\phi = -2\pi\beta N \pmod{2\pi}$, and lead to a \mathcal{PT} -symmetric tunneling Hamiltonian. The set of such points has measure zero and therefore, we ignore the positive thresholds that arise due to such accidental parity symmetry of the underlying $H_0(\lambda, \beta, \phi)$. We also note that when β is irrational, the tunneling is asymmetric and incommensurate with the lattice for any N , and the resultant \mathcal{PT} threshold is zero.

The smallest experimental realization of a “ \mathcal{PT} system without parity symmetry”, say in a waveguide array, will only require $N = 5$ waveguides, a dimer tunneling profile $t_k = J[1 + (-1)^k \lambda \cos \phi]$, and gain-loss potentials $\pm i\gamma$ at parity symmetric locations. This analytically solvable case also provides further insights into the results presented in this paper. It is straightforward to check that when $m_0 = 1$, the characteristic equation for the 5×5 Hamiltonian $H = H_0 + V$ has complex coefficients, and therefore, the \mathcal{PT} threshold at $m_0 = 1$ is zero.

When $m_0 = 1/\beta = 2$, the corresponding equation is purely real, and at small values of $\gamma \leq \gamma_{PT}$, the real spectrum is particle-hole symmetric [44]. The resulting threshold at which the eigenvalues transition from real to complex conjugate pairs is given by

$$\gamma_{PT}(\lambda, \phi) = 2J\sqrt{A_+} \left[1 - \sqrt{1 - \left(\frac{A_-}{2A_+} \right)^2} \right]^{1/2}, \quad (5)$$

where $A_{\pm} = 1 \pm \lambda^2 \cos^2 \phi$. It follows from Eq.(5) that the threshold γ_{PT} is insensitive to the tunneling modulation λ when $|\phi| \approx \pi/2$ and it is maximally suppressed when $\cos \phi = 0$. (See panel (c), Fig. 3.) It is also straightforward to show that the un-normalized, zero-energy, edge state eigenvector is given by $|f\rangle = (t_\phi^2, 0, -t_\phi, 0, 1)^T$ where $t_\phi = (1 + \lambda \cos \phi)/(1 - \lambda \cos \phi)$ is the ratio of tunneling amplitude on the second bond to the tunneling amplitude on the first bond. Thus, the edge state has nodes at integer multiples of $m_0 = 2$, is localized at the left end (right end) of the lattice when $t_\phi > 1$ ($t_\phi < 1$), and remains completely unaffected by the \mathcal{PT} potential.

Finally, we note that this paper is based on an effective, single-particle Hamiltonian that permits amplification and decay. *Prima facie*, the results predict the existence of topological insulators with positive \mathcal{PT} breaking threshold [38, 39], since our model makes no reference to the quantum statistics of the particle. In reality, however, amplification of a single degree of freedom is incompatible with Pauli principle. Thus, our results can apply to fermions only if the gain and loss are associated with the bulk Fermi sea, and not with a single quantum degree of freedom. In the bosonic case, amplification of a single degree of freedom is permitted and our results are directly applicable. We have also ignored two-body interactions; they become important only in the \mathcal{PT} -broken phase as the on-site intensity (light) or density (massive bosons) is amplified.

This work is supported by NSF DMR-1054020.

-
- [1] C.M. Bender and S. Boettcher, Phys. Rev. Lett. **80**, 5243 (1998).
- [2] C.M. Bender, D.C. Brody, and H.F. Jones, Phys. Rev. Lett. **89**, 270401 (2002).
- [3] C.M. Bender, Rep. Prog. Phys. **70**, 947 (2007) and references therein.
- [4] A. Guo, G.J. Salamo, D. Duchsne, R. Morandotti, M. Volatier-Ravat, V. Aimez, G.A. Siviloglou, and D.N. Christodoulides, Phys. Rev. Lett. **103**, 093902 (2009).
- [5] C.E. Rüter, K.G. Makris, R. El-Ganainy, D.N. Christodoulides, M. Segev, and D. Kip, Nat. Phys. **6**, 192 (2010).
- [6] L. Feng, M. Ayache, J. Huang, Y.-L. Xu, M.-H. Lu, Y.-F. Chen, Y. Fainman, and A. Scherer, Science **333**, 729 (2011).
- [7] Z. Lin, H. Ramezani, T. Eichelkraut, T. Kottos, H. Cao, and D.N. Christodoulides, Phys. Rev. Lett. **106**, 213901 (2011).
- [8] L. Feng, Y.-L. Xu, W.S. Fegadolli, M.-H. Lu, J.E.B. Oliveira, V.R. Almeida, Y.-F. Chen, and A. Scherer, Nat. Mater. **12**, 108 (2013).
- [9] A. Regensburger, C. Bersch, M.-A. Miri, G. Onishchukov, D.N. Christodoulides, and U. Peschel, Nature **488**, 167 (2012).
- [10] B. Peng, S.K. Ozdemir, F. Lei, F. Monifi, M. Gianfreda, G.L. Long, S. Fan, F. Nori, C.M. Bender, and L. Yang, Nat. Phys. **10**, 394 (2014).
- [11] M. Brandstetter, M. Liertzer, C. Deutsch, P. Klang, J. Schoberl, H.E. Tureci, G. Strasser, K. Unterrainer, and S. Rotter, Nat. Commun. **5**, 4034 (2014).
- [12] B. Peng, S.K. Ozdemir, S. Rotter, H. Yilmaz, M. Liertzer, F. Monifi, C.M. Bender, F. Nori, and L. Yang, Science **346**, 328 (2014).
- [13] L. Feng, Z.J. Wong, R.-M. Ma, Y. Wang, and X. Zhang, Science **346**, 972 (2014).
- [14] H. Hodaei, M.-A. Miri, M. Heinrich, D.N. Christodoulides, and M. Khajavikhan, Science **346**, 975 (2014).
- [15] O. Bendix, R. Fleischmann, T. Kottos, and B. Shapiro, Phys. Rev. Lett. **103**, 030402 (2009).
- [16] L. Jin and Z. Song, Phys. Rev. A **80**, 052107 (2009).
- [17] M. Znojil, Phys. Rev. A **82**, 052113 (2010).
- [18] Y.N. Joglekar and A. Saxena, Phys. Rev. A **83**, 050101(R) (2011).
- [19] D.D. Scott and Y.N. Joglekar, Phys. Rev. A **83**, 050102(R) (2011).
- [20] G. Della Valle and S. Longhi, Phys. Rev. A **87**, 022119 (2013).
- [21] S. Bose, Phys. Rev. Lett. **91**, 207901 (2003).
- [22] Y.N. Joglekar, C. Thompson, and G. Vemuri, Phys. Rev. A **83**, 063817 (2011).
- [23] M. Bellec, G.M. Nikolopoulos, and S. Tzortzakakis, Opt. Lett. **37**, 4504 (2012).
- [24] T. Kato, *Perturbation Theory for Linear Operators* (Springer-Verlag, Berlin, 1995).
- [25] Y.N. Joglekar, C. Thompson, D.D. Scott, and G. Vemuri,

- Eur. Phys. J. Appl. Phys. **63**, 30001 (2013).
- [26] Y.N. Joglekar, D.D. Scott, and A. Saxena, Phys. Rev. A **90**, 032108 (2014).
- [27] A. Mostafadazeh, J. Math. Phys. **43**, 205 (2002).
- [28] C.M. Bender, M.V. Berry, and A. Mandilara, J. Phys. A: Math. Gen. **35**, L467 (2002).
- [29] C.M. Bender and P.D. Mannheim, Phys. Lett. A **374**, 1616 (2010).
- [30] W.-P. Su, J.R. Schrieffer, and A.J. Heeger, Phys. Rev. Lett. **42**, 1698 (1979).
- [31] A.J. Heeger, S. Kivelson, J.R. Schrieffer, and W.-P. Su, Rev. Mod. Phys. **60**, 781 (1988).
- [32] D.R. Hoffstadter, Phys. Rev. B **14**, 2239 (1976).
- [33] P.G. Harper, Proc. Phys. Soc. London Sect. A **68**, 874 (1955).
- [34] S. Aubry and G. Andre, Ann. Isr. Phys. Soc. **3**, 133 (1980).
- [35] Y.E. Kraus, Y. Lahini, Z. Ringel, M. Verbin, and O. Zilberberg, Phys. Rev. Lett. **109**, 106402 (2012).
- [36] Y.E. Kraus and O. Zilberberg, Phys. Rev. Lett. **109**, 116404 (2012).
- [37] S. Ganeshan, K. Sun, and S. Das Sarma, Phys. Rev. Lett. **110**, 180403 (2013).
- [38] Y.C. Hu and T.L. Hughes, Phys. Rev. B **84**, 153101 (2011).
- [39] K. Esaki, M. Sato, K. Hasebe, and M. Kohmoto, Phys. Rev. B **84**, 205128 (2011).
- [40] H. Schomerus, Opt. Lett. **38**, 1912 (2013).
- [41] B. Zhu, R. Lu, and S. Chen, Phys. Rev. B **89**, 061202 (2014).
- [42] Y.N. Joglekar, D.D. Scott, M. Babbey, and A. Saxena, Phys. Rev. A **82**, 030103 (2010).
- [43] S. Klaiman, U. Gunther, and N. Moiseyev, Phys. Rev. Lett. **101**, 080402 (2008).
- [44] Y.N. Joglekar, Phys. Rev. A **82**, 044101 (2010).